

## Technical Notes

# Airflow Rate in the Quantitation of Volatiles in Air Streams by Solid-Phase Microextraction

Robert J. Bartelt\* and Bruce W. Zilkowski

National Center for Agricultural Utilization Research, Bioactive Agents Research Unit, USDA Agricultural Research Service, 1815 North University Street, Peoria, Illinois 61604

**A previously reported method for nonequilibrium quantitation of air-borne volatiles from air streams by solid-phase microextraction (SPME) was improved by broadening its scope. The original method was defined for the 100- $\mu$ m poly(dimethylsiloxane) fiber type for a wide range of analytes, sampling temperatures, and sampling times, but only for four specific airflow configurations. The present study extends the choice of volumetric airflow rates to a continuous range between 2 and 220 mL/min. Kinetics of absorption was characterized for 21 different airflow rates within this range using *n*-alkanes of 11–18 carbons. Nonlinear regression analysis was used to develop a relationship between airflow rate and absorption kinetics and then to integrate these results into the previous model. The overall model (with 8 fitted degrees of freedom and based on 2240 measurements) had an  $r^2$  value of 0.9972 and residual variability (RSD) of 9.75%, which compared favorably with the sampling precision of SPME (~5%). The method allows absolute quantitation by SPME for a broad range of analytes and sampling parameters without prior calibration of the individual fiber and regardless of whether equilibration is complete. Simulations are presented that demonstrate how the choice of airflow rate can affect quantitation.**

Solid-phase microextraction (SPME) is a versatile and increasingly popular method for sampling organic compounds. To us as biologists, an application of particular interest has been the quantitation of volatiles in air. However, many compounds of biological interest such as insect pheromones are relatively large and do not equilibrate with SPME fibers in a reasonable amount of time. We previously addressed this problem by developing a method for nonequilibrium quantitation in which the air-borne volatiles were sampled from an airstream.<sup>1</sup>

Central to this method was a mathematical description of the kinetics of absorption from an airstream (eq 1).<sup>1</sup> Here,  $M_{\text{fiber}}(t)$  is the mass of analyte in the fiber coating (ng) after sampling for time  $t$  (min),  $C_{\text{air}}$  is the concentration of analyte in the airstream

$$\frac{M_{\text{fiber}}(t)}{C_{\text{air}}} = K^* \left( 1 - \exp \frac{-AFt}{K^*} \right) \quad (1)$$

(ng/mL), and  $F$  is the volumetric airflow rate past the fiber (mL/min).  $K^*$  (mL) is the equilibrium ratio of mass absorbed by the fiber to concentration in the air ( $K^* = M_{\text{fiber}}(\infty)/C_{\text{air}}$ ); the value of  $K^*$  depends on the analyte and sampling temperature. (In the notation of Pawliszyn,<sup>22</sup>  $K^* = K_{\text{fg}} \times V_{\text{fiber}}$ ). The final parameter is  $A$ , which can be visualized as the fraction of the analyte in the airstream that has time to interact with the fiber, whereas  $(1 - A)$  is the fraction that is carried past the fiber without interacting. The value of  $A$  must be between 0 and 1; intuitively, rapid airflows would correspond to smaller values of  $A$ . Because  $A$  is in the exponential term, it is relevant to quantitation only when equilibration is not complete. In practice,  $M_{\text{fiber}}(t)$  is measured by gas chromatography (GC),  $F$  and  $t$  are set by the experimenter, and  $C_{\text{air}}$  is the target for quantitation. Once  $K^*$  and  $A$  are known by some means, then  $C_{\text{air}}$  can be calculated directly from the equation.

The idea of predicting  $K^*$  from other information was developed previously.<sup>3,4</sup> Our current model is given in eq 2. It was based

$$\log K^* = -3.5340 + G + (0.005062 - 0.00002853 \times \text{TEMP}) \times \text{LTPRI} \quad (2)$$

on nonlinear regression analysis of 1474 airstream SPME measurements for a variety of analytes and conditions.<sup>1</sup> Here, TEMP is the sampling temperature (°C) and LTPRI is the linear temperature-programmed retention index of the analyte on a nonpolar GC column.<sup>2,4</sup>  $G$  is a constant that depends only on functional group ( $G = 0.000$  for hydrocarbons, by definition;  $G = 0.100$  for methyl esters, and  $G = 0.360$  for alcohols). The nonzero values of  $G$  and the other three numerical constants in eq 2 are regression estimates.

Previously,<sup>1</sup>  $A$  was determined for four specific sampling situations: for volumetric airflow rates of 2 and 20 mL/min when sampling within a 1.5-mm inside diameter tube ( $A = 0.984$  and

\* Corresponding author: (phone) 309-685-4011; (e-mail) BartelRJ@Mail.NCAUR.USDA.gov.

(1) Bartelt, R. J.; Zilkowski, B. W. *Anal. Chem.* **1999**, 71, 92–101.

(2) Pawliszyn, J. *Solid-Phase Microextraction: Theory and Practice*; Wiley-VCH: New York, 1997.

(3) Bartelt, R. J. *Anal. Chem.* **1997**, 69, 364–372.

(4) Martos, P. A.; Sarullo, A.; Pawliszyn, J. *Anal. Chem.* **1997**, 69, 402–408.

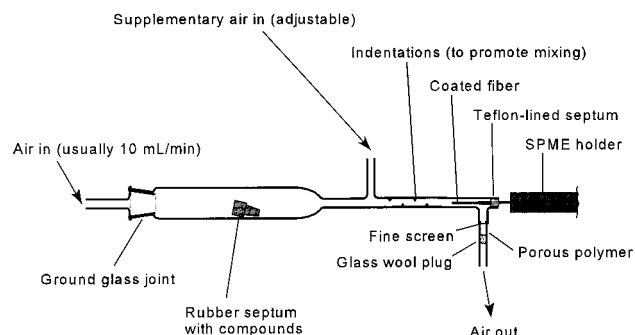


Figure 1. Diagrammatic view of apparatus used in this study.

0.276, respectively) and for flow rates of 20 and 200 mL/min for a 4.5-mm tube ( $A = 0.258$  and  $0.0512$ , respectively). To a very good approximation,  $A$  did not depend on analyte, temperature, or sampling time, but only on volumetric airflow rate. In the present study, kinetics of absorption was studied for 21 suitably spaced airflow rates to enable development of an equation for  $A$  analogous to that for  $K^*$ . The resulting model now allows SPME quantitation from airstreams with *any* volumetric airflow rate between 2 and 220 mL/min.

## EXPERIMENTAL SECTION

**Sampling Apparatus.** The sampling apparatus is shown diagrammatically in Figure 1 and was similar to that used earlier.<sup>1</sup> It allowed simultaneous measurement of the amount of analyte captured by the fiber and the concentration of analyte in the air to which the fiber was exposed. The analytes evaporated slowly into the airstream from a rubber serum vial stopper ("septum"). A supplementary airstream entered through a sidearm downstream of the septum, as explained below. The combined flow passed through a Teflon tube with indentations to promote mixing and then passed by the SPME fiber, which was positioned along the central axis of the glass sampling port and sealed in place by a Teflon-lined septum. Finally, the air exited through the sidearm of the sampling port, to which a trap containing porous polymer was attached. All analyte not absorbed by the fiber was captured by the trap.

The trap contained a 10-mm- by 3-mm-diameter plug of Super Q porous polymer (Alltech Associates, Deerfield, IL). The Super Q was held between a 300-mesh stainless steel screen (that was fused into the glass) and a plug of silanized glass wool. The trap was connected to the outlet tube with a short length of Teflon tubing. The fiber itself was positioned 29 cm downstream from the enlarged glass tube holding the septum and 21 cm downstream from the tube where the supplementary air entered. The internal diameter of the sampling port was 4.5 mm. The trap was located 3 cm downstream from the fiber. The whole apparatus was placed in an incubator which maintained the temperature at  $27 \pm 1$  °C.

**Septum Preparation.** Rubber septa (natural red rubber, 18 mm long  $\times$  10 mm in diameter, Wheaton, Millville, NJ) were extracted in a Soxhlet apparatus for 6 h with methylene chloride and then air-dried before use. They were loaded by applying a solution of *n*-alkanes (11–18 carbons) in hexane; thus both rapidly and slowly equilibrating compounds were represented. Amounts per septum were 2 mg each for alkanes of 11–15 carbons and 5

mg each for those of 16–18 carbons. Exact release rates were not known beforehand but were calculated later from the quantities captured by the fiber and trap. Loaded septa were aired in a hood overnight so that solvent would evaporate, and they were placed into the sampling apparatus with the chosen air flow at least 24 h before data collection began so that analyte emission would stabilize.

**Air Flow.** The air supply was a tank of dry, compressed air suitable for use with a GC FID. A pair of fine needle valves controlled airflow into the inlets of the sampling apparatus. All airflow measurements were made at the outlet (Figure 1) with an electronic flowmeter (Alltech Flow Check). The accuracy of the electronic meter was periodically checked with a bubble flowmeter. The airflow past the septum was set first, with the supplementary airflow off, and then the latter source was adjusted to give the desired total flow.

Twenty-one different rates of airflow past the fiber were employed, ranging from 2.1 to 219 mL/min and with consecutive settings differing by  $\sim 25\%$ . The flow past the septum was always 10 mL/min except when the total flow had to be less; thus, the supplementary airflow ranged from 0 to 209 mL/min. This arrangement was used because compound release from a rubber septum is affected by the speed of air movement. Maintaining a constant airflow past the septum whenever possible minimized the amount of time needed for the system to stabilize between changes in total flow and it also simplified the later calculations.

**Gas Chromatography.** A Hewlett-Packard 5890 series II instrument was used for all analyses. It was equipped with a flame ionization detector (FID), autosampler, cool on-column inlet, and HP Chem Station data system. The inlet was fitted with a 10-cm retention gap of deactivated fused-silica tubing (0.53-mm i.d., large enough to accommodate SPME injections). The narrow-bore analytical column (15-m DB-1, with 0.25-mm i.d. and 0.25- $\mu$ m film, J & W Scientific, Folsom, CA) was attached to the retention gap with a press-fit connector. The oven temperature program started at 50 °C for 1 min and then increased at 10 °C/min to 250 °C. Carrier gas was helium.

Response factors (integration units per nanogram) were determined from liquid samples. These samples were prepared gravimetrically, diluted to levels similar to those encountered in the study, and injected with the autosampler (five replications). Determinations were done at the beginning and again at the end of the study; these were consistent.

**SPME Sampling.** The SPME fibers were of the 100- $\mu$ m poly-(dimethylsiloxane) (PDMS) type (Supelco, Bellefonte, PA). The sampling time was always 30 min. a total of 3–11 samples were taken at each airflow rate. SPME sampling was delayed after changes were made to the airflow rate, so that the system had time to stabilize. This delay was at least 1 h when only the supplementary airflow was changed (all total flows between 10 and 219 mL/min) and at least 16 h when flow past the septum was changed (i.e., for flows less than 10 mL/min). The samples were analyzed by GC. The injection temperature was 200 °C, and injection duration was 30 s. The fiber was conditioned in another GC inlet for at least 2 min at 200 °C prior to reuse. Analyte amounts,  $M_{\text{fiber}}(t)$ , used in the subsequent statistical computations were calculated from the GC peak areas by using the detector response factors.

**Trap Collections.** The Super Q trap was operated continuously. Collected volatiles were recovered from the trap in early morning and again in late afternoon so that the collection intervals alternated between 8 and 16 h throughout the study. (The larger alkanes would not have been detected at all if the trap collections were as brief as the SPME collections.) To recover volatiles, the trap was removed and back-flushed into an autosampler vial with 500  $\mu\text{L}$  of hexane. Internal standard was added (40  $\mu\text{g}$  of pentacosane), and the sample was sealed, mixed, and analyzed by GC. Mass of analyte in the trap collection was calculated from the internal standard and FID response factors.

**Calculation of Concentrations.** Concentrations of analytes in the airstream were calculated as described in detail previously.<sup>1</sup> Briefly, the total amount of material passing through the system during a Super Q trapping interval was the sum of all of the SPME collections (ng) during that interval plus the amount in the trap, and mean flux (ng/min) from the septum for the period was that amount divided by the time interval. Theoretically,  $\log(\text{flux})$  for rubber septa decreases linearly with time because release is first order.<sup>5</sup> The logarithms of the observed mean flux values for the consecutive trapping intervals were used to determine the first-order release line for each of the eight analytes and for each of the six airflow rates past the septum (i.e., between 2.1 and 10 mL/min). The calculations were done by linear regression. These relationships then allowed the flux of any analyte to be calculated for any specific time after the septum was set up, and flux was readily converted to concentration ( $C_{\text{air}}$ , in ng/mL) by dividing by total flow rate (mL/min).

Emission rate from septa decreased noticeably over time for the smaller alkanes but remained essentially constant throughout the study for those of 15 or more carbons. Even for the most volatile alkane in the study (undecane), however, the change in concentration during any 30-min SPME sampling period was only  $\sim 1\%$ . Thus, the concentration experienced by the SPME fiber throughout any sampling period was effectively constant, as assumed in the kinetic model (eq 1). The concentration computed for the end of the SPME sampling period was the value for  $C_{\text{air}}$  used in the subsequent calculations.

**Regression Analysis.** The nonlinear least squares regression procedure (NLIN) of the Statistical Analysis System (SAS) program package<sup>6</sup> was used for model development. In all cases, the response variable of interest was  $M_{\text{fiber}}(t)/C_{\text{air}}$ , which is the amount of material captured by the fiber during sampling interval,  $t$ , normalized by the concentration in the air. The number of data points available was 766, representing the 8 alkanes ( $C_{11}$ – $C_{18}$ ) and 21 different flow rates (2.1–219 mL/min).

All of the regression models (eq 3) were based on the kinetic formula (eq 1), but the logarithmic transformation (base 10) was

$$\log \frac{M_{\text{fiber}}(t)}{C_{\text{air}}} = \log K^* + \log \left( 1 - \exp \left( -\frac{AFt}{K^*} \right) \right) + \epsilon \quad (3)$$

always applied to stabilize residual variance. In eq 3,  $\epsilon$  is the error

term, with mean equal to 0 and constant variance. If the data were not transformed, the standard deviation of  $\epsilon$  would be proportional to GC peak area, rather than constant, because of the nature of SPME-GC data.

In each case, expressions for  $A$  and  $K^*$  (or  $\log K^*$ ) were substituted into eq 3 before doing the regression calculations. Three different expressions for  $A$  were employed, and these are explained with the results. The expression for  $K^*$  given in eq 2 was not used directly. Rather, the parameters for  $K^*$  were estimated anew from the current data set for each new model for  $A$ , to explore for any unexpected interactions between  $K^*$  and  $A$  or differences in  $K^*$  values between data sets. ( $K^*$  for this study required just two parameters instead of five because only one temperature and one chemical functional group were involved). In fact, the estimates for  $K^*$  from this study and the previous one were in excellent accord and no complicating interactions were evident. Later, when the current and previous data sets were combined, the parameters for  $K^*$  were again recalculated to take advantage of the entire data set. For each model, all parameters describing  $K^*$  and  $A$  were fitted simultaneously. Residual error for each model was expressed as the relative standard deviation (RSD) of the untransformed response variable.

## RESULTS AND DISCUSSION

**Expressions for  $A$  with the Current Data Set.** The first model for  $A$  (eq 4) simply allowed each of the 21 different flow

$$A = A_i \quad i = 1, \dots, 21 \quad (4)$$

rates (represented by  $i$ ) to have a unique  $A$  value.

The estimated  $A$  values are plotted in Figure 2 versus volumetric airflow rate and each was based on between 24 and 88 data points. Derivation of eq 1 imposed the restriction that  $A$  must always be between 0 and 1,<sup>1</sup> but the regression model imposed no such restriction. That all of the fitted  $A$  values fell within this range gave credibility to the underlying kinetic model and the experimental approach. The fit of the model was quite good (RSD = 6.11%) and very close to the variability inherent in SPME sampling ( $\sim 5\%^{1-3}$ ). The overall model, with 23 fitted degrees of freedom (21 for  $A$  and 2 related to  $K^*$ ), explained 99.5% of the variance in the data set. The plotted  $A$  values suggested a curve, and the subsequent models sought to describe it mathematically.

From Figure 2 and theoretical considerations, the function for  $A$  would be expected to decrease asymptotically to 0 as the volumetric flow rate increased without bound. However, it was not clear how the curve should behave as it approached  $A = 1$  at low flows. One possibility is that at some sufficiently slow flow rate, all of the airstream analyte molecules would be able to contact the fiber (i.e.,  $A = 1$ ); however, still slower flows could not make  $A$  exceed its maximum. This situation would result in a plateau-shaped curve. A modified power function was chosen empirically as a reasonable form for representing this possibility (eq 5). Here,

$$A = \min(1.00, UF^W) \quad (5)$$

$A$  is the lesser of two quantities: 1.00 and the value of the power function (which might conceivably be greater than 1 for some

(5) McDonough, L. M. In *Naturally Occurring Pest Bioregulators*; Hedin, P. A., Ed.; ACS Symposium Series 449; American Chemical Society: Washington, DC, 1991; Chapter 8.

(6) SAS Institute, Inc. *SAS User's Guide: Statistics*, Version 6 ed.; SAS Institute, Inc.: Cary, NC, 1990.

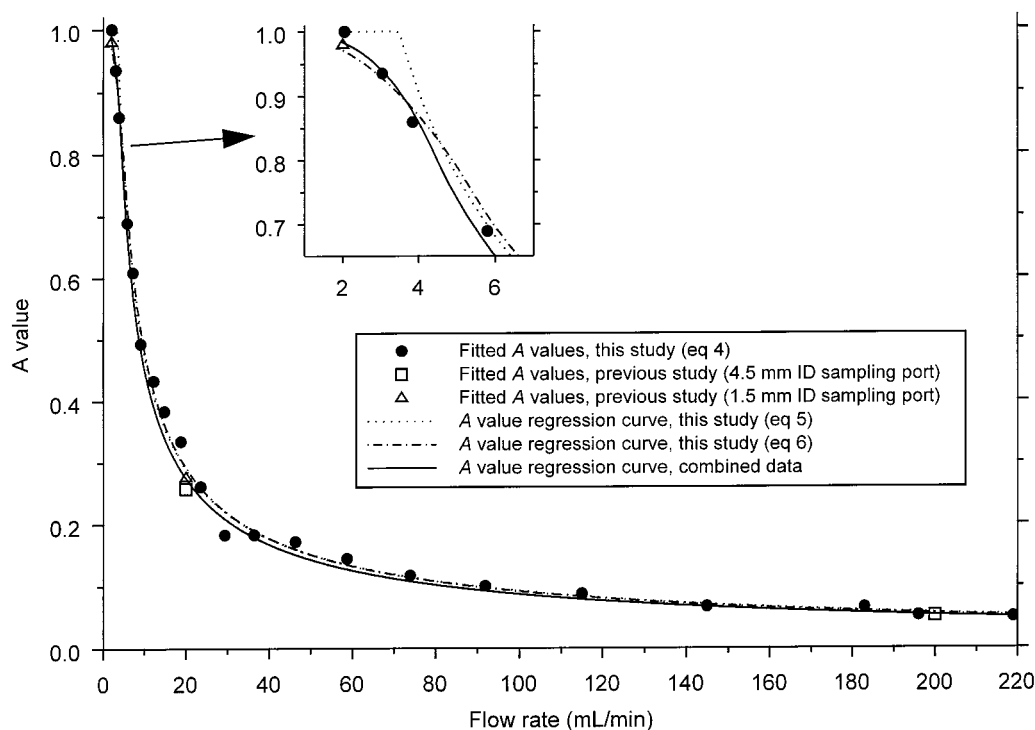


Figure 2. Plots of *A* value versus airflow rate for individual experimental determinations and various fitted curves.

Table 1. Summary of Parameter Values and Statistics for Combined Model, Compared to the Previous Model

parameter	combined data sets	previous data set <sup>1</sup>
<b>Parameters Related to <math>K^*</math> (See Eq 2) (<math>\pm</math>SE)</b>		
(Form: $\log K^* = P + G + (Q_1 + Q_2 \times \text{TEMP}) \times \text{LTPRI}$ )		
<i>P</i>	-3.5244 ( $\pm 0.0090$ )	-3.5340 ( $\pm 0.0092$ )
<i>Q</i> <sub>1</sub>	0.005052 ( $\pm 0.000011$ )	0.005062 ( $\pm 0.000011$ )
<i>Q</i> <sub>2</sub>	-0.00002849 ( $\pm 0.00000027$ )	-0.00002853 ( $\pm 0.00000026$ )
<i>G</i> (hydrocarbons)	0.00 (by definition)	0.00 (by definition)
<i>G</i> (methyl esters)	0.095 ( $\pm 0.0046$ )	0.100 ( $\pm 0.0045$ )
<i>G</i> (alcohols)	0.356 ( $\pm 0.0046$ )	0.360 ( $\pm 0.0046$ )
<b>Parameters and Results Related to <i>A</i> (see Eq 6) (<math>\pm</math>SE)</b>		
<i>U</i>	2.34 ( $\pm 0.027$ )	
<i>W</i>	-0.715 ( $\pm 0.0035$ )	
<i>Z</i>	4.4 ( $\pm 0.19$ )	
<i>U</i> <sub>slow</sub>	0.00199 (calculated)	
<i>W</i> <sub>slow</sub>	3.08 (calculated)	
<i>A</i> at 2 mL/min (1.5-mm-i.d. port)	0.983 (predicted)	0.984 ( $\pm 0.012$ )
<i>A</i> at 20 mL/min (1.5-mm-i.d. port)	0.275 (predicted)	0.276 ( $\pm 0.0026$ ),
<i>A</i> at 20 mL/min (1.5-mm-i.d. port)	0.275 (predicted)	0.258 ( $\pm 0.0013$ )
<i>A</i> at 200 mL/min (4.5-mm-i.d. port)	0.0530 (predicted)	0.0512 ( $\pm 0.0006$ )
<b>Summary Statistics and Properties of Models</b>		
data points	2240	1474
fitted parameters	8	9
RSD, %	9.75	9.46
<i>r</i> <sup>2</sup>	0.9972	0.9981

flows). In the power function, *F* is the measured volumetric airflow rate and *U* and *W* are constants to be estimated. The number of fitted degrees of freedom involving *A* was reduced from 21 to just 2 with this model. The estimated values of constants *U* and *W* were 2.427 and -0.7095, respectively, and the residual error was 8.08% RSD. The total number of fitted degrees of freedom was 4

(including the two for  $K^*$ ), and the *r*<sup>2</sup> value was 99.2%. The fitted curve of *A* versus flow rate is plotted in Figure 2. The flow rate at which the curve reached *A* = 1 was 3.5 mL/min. The increase in residual error over the model using eq 4 was due primarily to the scatter of *A* values about the curve. Residual analysis did not indicate a systematic departure from the curve except for the very slow flow rates (Figure 2, inset). The *A* values did not rise sharply to a plateau with decreasing flow but instead approached 1.0 gradually. It is suggested that diffusion along the axis of the tubing became relatively important at the slow flow rates and "softened" the shape of the curve for *A*. There appeared to be an inflection point in the curve at some flow rate around 4 or 5 mL/min.

The regression model was modified to improve the fit at slow flows. The section of the graph of *A* versus air flow for slow flow rates was modeled as a second power function that would approach 1.00 as flow approached 0. This second function was constrained to be continuous with the first and to be smooth (i.e., the first derivatives were equal) where they met. These conditions are summarized below (eqs 6). Here, *Z* is the flow rate at which

$$A = UF^W \quad \text{if } F \geq Z, \quad \text{or}$$

$$A = 1 - U_{\text{slow}}F^{W_{\text{slow}}} \quad \text{if } F < Z,$$

$$\text{such that } UZ^W = 1 - U_{\text{slow}}Z^{W_{\text{slow}}} \quad \text{and}$$

$$\frac{d(UF^W)}{dF} = \frac{d(1 - U_{\text{slow}}F^{W_{\text{slow}}})}{dF} \quad \text{when } F = Z \quad (6)$$

the two curves meet and is a parameter to be estimated. The conditions expressed in the last two lines fix the values of *U*<sub>slow</sub> and *W*<sub>slow</sub>, once *U*, *W*, and *Z* are known. Thus, there are just three degrees of freedom to be fitted relating to *A*. It can be shown



Table 2. Summary of Properties, Measurements, and Results for the Alkanes in the Study

no. of carbons	LTPRI	range of amts captured by fiber (ng)	range of concns in air near fiber (ng/mL)	fitted $K^*$ (27 °C)	
				combined model	previous data set only <sup>1</sup>
11	1100	0.66–535	0.046–36	15.4	15.3
12	1200	15–1260	0.39–32	41.4	41.2
13	1300	47–1230	0.48–16	111	111
14	1400	35–661	0.20–5.8	298	297
15	1500	18–323	0.076–2.5	798	798
16	1600	6–105	0.02–0.77	2140	2140
17	1700	2.2–37	0.0088–0.27	5740	5750
18	1800	0.80–14	0.0032–0.10	15400	15400

that these equations (6) determine the relationships presented for  $W_{\text{slow}}$  and  $U_{\text{slow}}$  (eqs 7). The estimates of  $U$  and  $W$  were 2.528

$$W_{\text{slow}} = \frac{-UWZ^W}{1 - UZ^W} \quad U_{\text{slow}} = \frac{1 - UZ^W}{Z^{W_{\text{slow}}}} \quad (7)$$

and  $-0.7203$ , respectively, and the inflection point occurred at a flow of  $Z = 5.40$  mL/min. From these values,  $U_{\text{slow}}$  and  $W_{\text{slow}}$  were calculated to be 0.006 46 and 2.17, respectively. The residual error was 7.72% RSD, a slight decrease from the previous model because of the improved behavior at slow flows. The total number of fitted degrees of freedom was 5 (including two for  $K^*$ ), and value of  $r^2$  was 99.3%. From Figure 2, this formulation gave a reasonable description for the behavior of  $A$  over the entire experimental range of flow rates.

**Regression Model for Combined Data Sets.** The 766 data points from the present study and the 1474 from the previous study<sup>1</sup> were combined and the regression analysis was repeated, using the final model (eq 6) for  $A$ . The overall calculated curve for  $A$  versus airflow rate is plotted in Figure 2. The estimated parameters, their standard errors, and summary statistics are compared in Table 1 for the combined and previous models. The fitted  $K^*$  values for the alkanes are similarly compared in Table 2. (Also given in Table 2 are the LTPRI values and the ranges of fiber amounts and vapor-phase concentrations encountered during the study.)

In Table 1, the slightly higher residual error with the combined model (9.75% RSD instead of 9.46% for the previous model) was due almost entirely to one estimate of  $A$  from the earlier data set: The  $A$  value for 20 mL/min flow through the 4.5-mm-i.d. sampling port was lower (0.258) than that estimated solely from the new data set (0.292, with model constraints as in eq 6). The earlier  $A$  value had a great deal of influence in the combined model because it was based on so many (933) data points. Nevertheless, the magnitude of the difference is relatively small, and there is good overall agreement between the present and previous data sets. Combining them can be expected to give the most reasonable approximations for both  $A$  and  $K^*$ .

**Possible Interactions and Minor Effects.** The actual SPME absorption process is undoubtedly more complicated than the final model would indicate. There are physical chemical reasons why  $A$  might depend on analyte size or sampling temperature, for example. Careful examination of the data indicates that such effects are minimal, and for the sake of simplicity they are ignored. Still, future “fine-tuning” may be required for utmost accuracy.

Table 3. Summary of Final Quantitation Model

$$\text{equation: } \frac{M_{\text{fiber}}(t)}{C_{\text{air}}} = K^* \left( 1 - \exp \frac{-AFt}{K^*} \right)$$

where

$\log K^* = -3.524 + G + (0.00505 - (0.0000285 \times \text{TEMP})) \times \text{LTPRI}$

and  $A = 1 - 0.00199 \times F^{3.08}$  if  $F \leq 4.4$

or  $A = 2.34 \times F^{-1.715}$  if  $F > 4.4$

symbols and units:

$M_{\text{fiber}}(t)$  is amount of analyte in fiber (ng, measured by GC) after  $t$  min of sampling

$C_{\text{air}}$  is the concentration of analyte in the airstream (ng/mL). (This is the unknown quantity that is to be calculated.)

$F$  is the volumetric airflow rate past the fiber (mL/min)

$t$  is the sampling duration (min)

$K^*$  is the calibration factor (mL) (calculated from TEMP and LTPRI and functional group information)

$A$  is the efficiency factor (dimensionless) (calculated from  $F$ )

TEMP is the sampling temperature (°C)

LTPRI is the linear temperature-programmed retention index of the analyte on a nonpolar column (dimensionless)

$G$  is the functional group correction term (dimensionless):

= 0.00 for hydrocarbons

= 0.10 for methyl esters

= 0.36 for alcohols

(values for additional functional groups given in ref 3)

**Diameter of Sampling Port.** Two sampling port internal diameters have been used, 1.5 and 4.5 mm. As shown in Figure 2,  $A$  values from both of these agreed well. Apparently port diameter has a minimal effect on the value of  $A$  or on quantitation (at least within the range of 1.5–4.5 mm). It was previously discussed why this might be so.<sup>1</sup> Nevertheless, unless there is a compelling reason to do otherwise, using a sampling port of close to 4.5-mm i.d. would seem prudent until a more systematic study is done.

**Practical Quantitation.** The apparatus for routine quantitation would differ from that in Figure 1. No Super Q trap would be required, and the SPME fiber would simply be inserted into the open end of the tube through which the airstream was emerging. Typically, the airstream would first pass through a vessel containing the volatile source. A key concept is that once the system stabilizes, the rate of analyte emission from the volatile source (ng/min) will be equal to the rate at which it emerges from the tube, and this can now be measured.

Table 3 summarizes the equations and parameter values for the final model. To use these,  $\log K^*$  is first calculated from sampling temperature, analyte LTPRI, and analyte functional group information. Values of  $G$  for additional functional groups are also

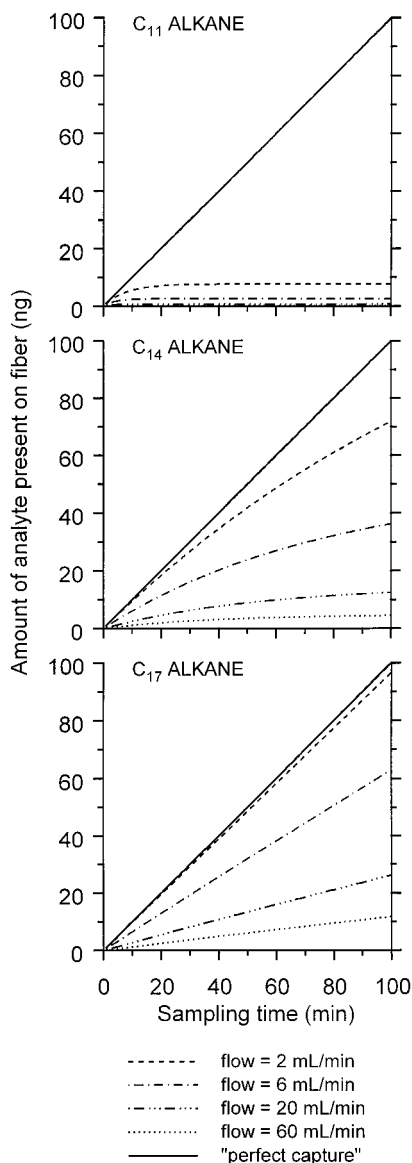


Figure 3. Simulation under conditions of constant analyte flux (always 1 ng/min). Curves represent amounts of analyte accumulated by SPME fiber at various sampling times. Amounts cannot be above the diagonal line representing "perfect capture".

available.<sup>3</sup> After conversion of  $\log K^*$  to its antilog and calculation of  $A$  from airflow rate, these values are substituted into the main equation, along with airflow rate and sampling time. This fully determines the proportionality factor for calculating  $C_{\text{air}}$  directly from  $M_{\text{fiber}}(t)$ . The final required item of information for each analyte is the GC detector response factor so that peak areas can be converted to nanograms. The overall result is that the absolute concentration of analyte in the airstream can be calculated directly from GC peak area. Multiplication of this concentration (ng/mL) by volumetric flow rate (mL/min) gives analyte flux (ng/min), which is often of greater practical interest. Because the 100- $\mu\text{m}$  PDMS fibers are manufactured so uniformly and change little over time, all fibers of this type are expected to give essentially the same answers.<sup>7</sup> The calculations are cumbersome by hand but can easily be automated, for example, in macro programs running on GC data stations.

(7) Martos, P. A.; Pawliszyn, J. *Anal. Chem.* **1997**, *69*, 206–215.

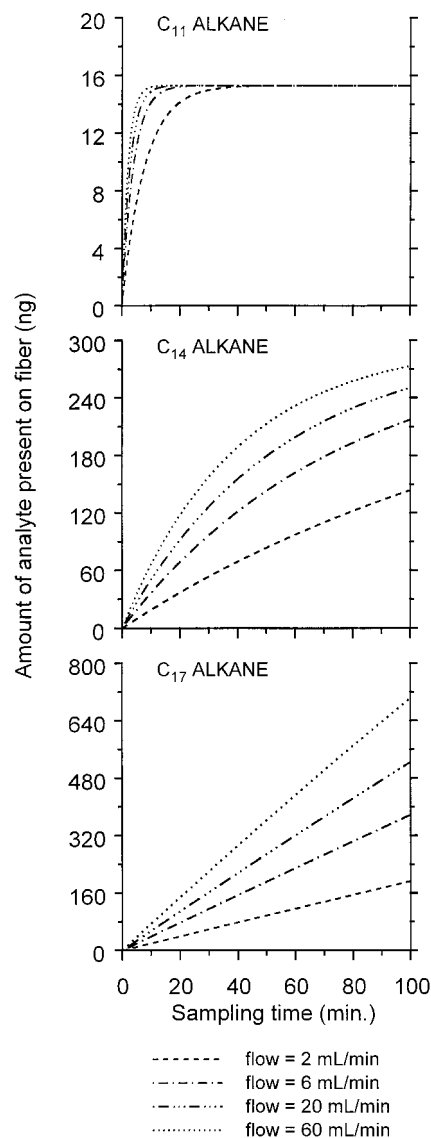


Figure 4. Simulation under conditions of constant concentration (always 1 ng/mL in airstream). Curves represent amounts of analyte accumulated by SPME fiber at various sampling times.

This approach to quantitation has been used to measure emission rates (fluxes) of fungal volatiles from cultures,<sup>8</sup> delivery rates of synthetic and natural volatile mixtures to insect behavioral bioassays,<sup>9</sup> and release rates of synthetic insect pheromones from slow-release formulations.<sup>10</sup> It is also anticipated that quantitation from airstreams could be automated in the future, using apparatus similar to that already reported.<sup>11</sup>

**Simulations.** The fiber amounts and concentration data in Table 2 indicate that remarkable sensitivity is possible with SPME. Simulations using the kinetic model (eq 1) can indicate the expected level of sensitivity and can guide the choice of sampling conditions to maximize sensitivity. The following two examples deal specifically with volumetric airflow rate.

The first is a hypothetical volatile source that emits a constant amount of chemical per unit time (a constant flux), regardless of

(8) Bartelt, R. J.; Wicklow, D. T. *J. Agric. Food Chem.* **1999**, *47*, 2447–2454.

(9) Bartelt, R. J.; Zilkowski, B. W. *J. Chem. Ecol.* **1998**, *24*, 535–558.

(10) Cossé, A. A.; Bartelt, R. J. *J. Chem. Ecol.* **2000**, *26*, 1735–1748.

(11) Eisert, R.; Pawliszyn, J.; Barinshteyn, G.; Chambers, D. *Anal. Commun.* **1998**, *35*, 187–189.

how fast air is flowing past it. (Pheromone emission from an insect could be approximated by this model.) The source for Figure 3 is emitting undecane, tetradecane, and heptadecane, each at a rate of 1 ng/min. The graphs show the mass of each material present on the fiber at any sampling time up to 100 min, for any of four flow rates (2, 6, 20, and 60 mL/min). The diagonal line in each graph represents "perfect capture" by the fiber (100 ng at 100 min); no points can be above this line.

For the  $C_{11}$  compound, equilibration is rapid at any flow rate, but the fiber amounts are all relatively low. The amount is highest for the slowest airflow because the emitted analyte is diluted by the least air (constant flux implies that concentration, and therefore, equilibrium fiber amount is inversely proportional to volumetric airflow rate). The plots for  $C_{11}$  show little influence of  $A$  because equilibration is rapid. For  $C_{17}$ , the amounts of material captured are greater and the plots continue to rise at all sampling times; in no case is equilibrium reached. These graphs demonstrate primarily the influence of  $A$ . At 2 mL/min, where  $A$  is 0.98, nearly perfect capture of the compound is achieved, but higher flow rates and the resulting smaller  $A$  values lead to less material being collected. As long as  $K^*$  is "large" (e.g., greater than 1000), the plots for *any* compound would appear just as for the  $C_{17}$  hydrocarbon; the actual value of  $K^*$  would be irrelevant. The graphs for  $C_{14}$  represent a transition from a situation dominated by  $K^*$  to one that is dominated by  $A$ . The practical guidance in

this case would be to set the airflow rate as *slow* as possible to get maximum sensitivity for all of the compounds.

The second simulation example is one in which the *concentration* of the three hydrocarbons is always constant, regardless of airflow rate. This would occur, for example, if air were being drawn from a large room at some set rate through a tube where the SPME fiber was located. For Figure 4, the concentration of each of the hydrocarbons is assumed to be 1 ng/mL. As before,  $C_{17}$  is always captured in the largest amount. However, in this situation, dilution does not occur; for each compound, all plots are progressing toward the same equilibrium value (although only  $C_{11}$  would reach it within 100 min). Of particular interest is that, for any compound, the amount on the fiber at any time is highest for the *fastest* (instead of slowest) flow rate. In this case, the quicker equilibration caused by rapid airflow more than compensates for the lower efficiency ( $A$  value) associated with fast flow. The practical guidance in this situation would be to set the airflow rate as *fast* as possible to get maximum sensitivity. Appropriate choice of conditions is not always intuitively obvious, and simulations such as those above can provide helpful insight.

Received for review February 2, 2000. Accepted June 2, 2000.

AC000101F